arXiv:astro-ph/0102079v1 5 Feb 2001

Dynamical Friction in dE Globular Cluster Systems

Jennifer M. Lotz [1], Rosemary Telford [2], Henry C. Ferguson [3]

Bryan W. Miller [4], Massimo Stiavelli [3] and Jennifer Mack [3]

ABSTRACT

The dynamical friction timescale for globular clusters to sink to the center of a dwarf elliptical galaxy (dE) is significantly less than a Hubble time if the halos have King-model or isothermal profiles and the globular clusters formed with the same radial density profile as the underlying stellar population. We examine the summed radial distribution of the entire globular cluster systems and the bright globular cluster candidates in 51 Virgo and Fornax Cluster dEs for evidence of dynamical friction processes. We find that the summed distribution of the entire globular cluster population closely follows the exponential profile of the underlying stellar population. However, there is a deficit of bright clusters within the central regions of dEs (excluding the nuclei), perhaps due to the orbital decay of these massive clusters into the dE cores. We also predict the magnitude of each dE's nucleus assuming the nuclei form via dynamical friction. The observed trend of decreasing nuclear luminosity with decreasing dE luminosity is much stronger than predicted if the nuclei formed via simple dynamical friction processes. We find that the bright dE nuclei could have been formed from the merger of orbitally decayed massive clusters, but the faint nuclei are several magnitudes fainter than expected. These faint nuclei are found primarily in $M_V > -14$ dEs which have high globular cluster specific frequencies and extended globular cluster systems. In these galaxies, supernovae-driven winds, high central dark matter densities, extended dark matter halos, the formation of new star clusters, or tidal interactions may act to prevent dynamical friction from collapsing the entire globular cluster population into a single bright nucleus.

Subject headings: dark matter – galaxies: dwarf – galaxies: kinematics and dynamics – galaxies: star clusters

[1]Henry A. Rowland Department of Physics and Astronomy, Johns Hopkins University, 3400 N. Charles St., Baltimore, MD 21218; jlotz@pha.jhu.edu

[2]Department of Physics and Astronomy, University of Wales, Cardiff, Wales, U.K. CF2 3YB; TelfordRE@Cardiff.ac.uk

[3]Space Telescope Science Institute, 3700 San Martin Dr., Baltimore, MD 21218; ferguson@stsci.edu, mstiavel@stsci.edu, mack@stsci.edu

[4]Gemini Observatory, Casilla 603, La Serena, Chile; bmiller@gemini.edu

1. Introduction

Dwarf elliptical galaxies (dEs) are small, low mass ($\sim 10^9\ M_\odot$), low luminosity ($M_B > -16$), elliptical shaped galaxies with little or no gas and no ongoing star formation. They are the most common type of galaxy in the local universe, outnumbering giant galaxies and dwarf irregulars in nearby clusters (Binggeli, Sandage & Tammann 1985; Ferguson & Sandage 1988) and appearing in roughly the same numbers as dwarf irregulars in low-density environments such as the Local Group (Grebel 1997). In "bottom-up" hierarchical merging scenarios of galaxy formation, dwarf-sized objects are the fundamental building blocks of larger galaxies. If dEs formed via gravitational collapse onto compact dark matter halos, then they may present a fossil record of the seeds of giant galaxy formation. On the other hand, if dEs form from the tidal debris of galaxy collisions (Mirabel, Dottori, & Lutz 1992; Barnes & Hernquist 1992; Hunsberger, Charlton, & Zaritsky 1996), then they are but a side-effect of giant galaxy formation. A better understanding of dE star formation histories and the nature of dE dark matter halos can help distinguish between these different formation scenarios.

The variation of structure and chemical abundance with dE galaxy mass is most simply understood as the result of rapid star-formation within a dark matter halo, terminated by supernova-driven winds (Dekel & Silk 1986). However, the varied star-formation histories of the Local Group dwarf spheroidal (dSph) and dE galaxies suggest that the picture is more complicated, at least for these nearby examples (Grebel 1997). Constraints on the ages and metallicities of the more extensive dE populations in nearby clusters are somewhat ambiguous, although integrated optical and infrared colors and spectral features (Thuan 1985; Caldwell & Bothun 1987; James 1994; Bothun & Mould 1988) suggest that dEs are primarily old, metal-poor populations with a few exceptions. Environmental effects, such as tidal interactions, galaxy harassment, and ram-pressure stripping, may play a large role in the transformation of gas-rich proto-dEs into the gas-poor dEs and regulate their star formation processes (e.g. Moore, Lake & Katz 1998).

Brighter than $M_B = -14$, over 50% of dEs possess compact stellar nuclei (Sandage, Binggeli & Tammann 1985). The nuclei for the most part appear as unresolved sources (even at HST resolution) projected very near the isophotal center of the galaxy. These could, at least in principle, be the merged conglomeration of globular clusters that have spiraled into the centers of the galaxies (Tremaine, Ostriker, & Spitzer 1975). However, there are reasons to suspect that dE nucleus formation may not be so straight-forward. Within the Virgo and Fornax clusters, the spatial distributions of the dE,N galaxies and dE galaxies brighter than $M_B = -14$ are significantly different. The dE,N galaxies follow the radial distribution of the early-type (E and S0s) giant galaxies, while the bright dEs (no N) galaxies follow the radial distribution of the spirals and irregulars (Ferguson & Sandage 1989). It is difficult to see how a purely internal process for the formation of dE nuclei such as dynamical friction could mimic such an environmental effect. Also, the dE,N galaxies have a somewhat higher globular cluster specific frequency S_N (the number of clusters normalized to galaxy luminosity $M_V = -15$) than non-nucleated dE, even when the nuclei are not counted as clusters, which also suggests a different origin for the two galaxy types (Miller

et al. 1998, 2001). And finally, dynamical friction calculations suggest that if nuclei are formed by the merger of decayed clusters, faint dEs should be more likely to be nucleated because they have shorter cluster decay times for fixed cluster mass; however it is the bright dEs which are more likely to be nucleated (Sandage, Binggeli, & Tammann 1985). An alternative scenario to dynamical friction as the dE nuclear formation mechanism suggests that dE nuclei are the remnants of the last burst of star-formation during the transition from dwarf irregulars (dIs) to dEs (Davies & Phillips 1988).

Globular cluster formation is often associated with periods of vigorous star formation, such as the initial monolithic gravitational collapse of proto-galaxies (Harris 1991) or starbursts sparked by galaxy mergers and interactions (e.g. the Antennae, Whitmore & Schweizer 1995). The characteristics of the resulting cluster system record the time since formation and the properties of the host galaxy. The colors of the clusters reflect their ages and abundances, which constrain the star formation history of the host galaxy. The current number of clusters depends on the globular cluster formation efficiency and the cluster destruction efficiency of the host galaxy, which may vary with Hubble type and galaxy mass. The globular cluster specific frequency S_N is a function of Hubble type and may give insight into the formation of the globular cluster system (GCS) and host galaxy. The present spatial distribution of the clusters traces the host galaxy's gravitational potential and dark matter component as well as constrains the initial radial distribution and kinematics of the cluster population.

In the Local Group, observations of the dSph GCSs have presented some interesting puzzles. Recent observations of the globular cluster systems of the Local Group dwarf spheroidals Sagittarius and Fornax have shown a significant age spread in these systems (Buonanno et al. 1999; Fusi Pecci et al. 1995; Montegriffo et al. 1998). The epoch of globular cluster formation for these two galaxies lasted for least 3-7 Gyr and the youngest globular cluster is $\sim$ 5-7 Gyr old. These galaxies also have extremely high specific frequencies ($S_N > 25$) - in other words, they have more clusters than expected for such faint, low mass systems (van den Bergh 1995). Finally, despite their short dynamical friction timescales, both Fornax and Sagittarius have retained extended globular systems (Oh, Lin, & Richer 2000).

We have embarked on a Hubble Space Telescope (HST) snapshot survey of globular cluster systems in dE galaxies in nearby clusters and groups. A primary goal of the study is to determine whether the globular cluster specific frequency is high ($S_N \gtrsim 3$), like giant ellipticals, or low ($S_N < 1$), like dwarf irregulars. The relatively high values of S_N found in the first half of our survey (Miller et al. 1998) suggest that dEs (and especially nucleated dEs) are not simply the faded remnants of dwarf irregular galaxies that have been stripped of their gas. In this paper, we consider the constraints on dE evolution provided by their nuclear properties and the spatial distributions of their globular clusters and search for evidence of dynamical friction processes.

A globular cluster orbiting a galaxy will experience a drag force due to its gravitational interaction with the surrounding stars and dark matter. Over time, this "dynamical friction" (Chan-

drasekhar 1943) will cause the globular cluster to lose energy and spiral in toward the bottom of the gravitational well. The timescale over which this happens depends on the mass of the globular cluster, its orbit, and the velocity distribution function of the particles with which it is interacting. In §3 we show that for the simplest assumptions – that the globular clusters began with the same radial distribution as the stars, that their orbits are isotropic, and that the dark matter distribution is an isothermal or King sphere – the dynamical friction timescales are significantly shorter than a Hubble time. In §4 we then examine the radial distribution of globular clusters in the 51 dE galaxies in our HST snapshot survey for evidence of these dynamical friction processes. We find that the bright clusters (excluding the nuclei) show a 4 σ depletion relative to an exponential radial profile, consistent with the orbital decay of these clusters into the dE centers. In §5 we simulate the formation of dE nuclei via dynamical friction. Our simulations for the fainter dEs predict nuclei several magnitudes brighter than observed. These dEs have high globular cluster specific frequencies and extended globular cluster systems but very short predicted decay timescales. We discuss in §6 the processes which may be working against the orbital decay of the globular clusters into a single bright nucleus in the faintest dEs.

2. Observations and Data Analysis

HST WFPC2 snapshot images (HST Cycle 6 6352 and Cycle 7 7377 programs) in F555W (2 $\times$ 230 seconds) and F814W (300 seconds) were taken of each galaxy, with the galaxy centered on chip 3. The DAOFIND detection algorithm was run on the F555W image and circular aperture photometry of all detected objects was done using a 3 pixel radius aperture. The average aperture corrections for the WF chips are -0.275 $\pm$ 0.014 for F555W and -0.307 $\pm$ 0.015 for F814W. The $V-I$ colors ($0.5 < V-I < 1.5$) and size (FWHM < 2.5 pixels) were used to select globular cluster candidates. Objects detected on chips 2 and 4 that met our selection criteria were considered background/foreground objects and were used to determine the background/foreground contamination of chip 3. All of the dE nuclei in the sample were compact enough to be considered globular cluster candidates, and, thus, were not well resolved even with the high resolution of HST WFPC2 ($\sim 0.1\,''$ per pixel). We assumed distance moduli of 31.2 for the Virgo Cluster, 31.4 for the Fornax Cluster, and 30.3 for the Leo Group. More details on the data reduction and object selection can be found in Miller et al. (1998).

Assuming that the globular clusters have a luminosity function (LF) similar to the Local Group GCLF, we detect 85-90% of the clusters in Virgo and Fornax (down to $M_V \sim -6$) (Figure 1a) and 98% of the clusters in Leo. Therefore we multiply the total number of Virgo and Fornax globular cluster candidates by 1.15 to correct for incompleteness. However, because we wish to obtain the radial profiles of the globular cluster systems, we must also determine the completeness as a function of radius from the center of the host galaxy. Dwarf galaxies are generally of low surface brightness, $\mu_o > 21$ V magnitudes/arcsec^2 (Binggeli & Cameron 1991), so we expect the globular cluster detection efficiency to worsen significantly only in the central regions of the dE. Simulations

of a GCS for a V=15.2 ($M_V = -16$ at Virgo) dE show that the cluster detection rate is $\sim 70\%$ for $r < r_0$ and is $> 95\%$ for $r > 3r_0$ (Figure 1b). It is the faint clusters which are missed and clusters brighter than $M_V = -7.0$ at the distance of Virgo and Fornax are detected at all radii.

Zero to twenty-five globular cluster candidates were found for each galaxy (Tables 1 and 2). The IRAF task ELLIPSE was used to determine the center, exponential scalelength r_0, and angle of orientation for each galaxy. The isophotal radial distance (the semi-major axis length of the intersecting galactic isophote) for each globular cluster candidate was calculated. Because each galaxy possesses only a small number of globular cluster candidates, a composite globular cluster radial distribution was created by scaling each globular cluster system by the host galaxy's exponential scalelength. Before summing the radial profiles of the entire dE sample, the profiles were corrected for background/foreground object contamination by subtracting the estimated number of background objects per radial bin for each dE. The summed profile was then corrected for radial incompleteness effects.

3. Dynamical Friction Timescales

The observed radial distribution of a galaxy's GCS depends on 1) the initial radial distribution; 2) the cumulative effects of dynamical friction (which in turn depend on the host galaxy's gravitational potential well and dynamical structure, as well as the mass distribution of the clusters); and 3) the efficiency of destruction mechanisms near the galaxy's center such as bulge and disk shocking. Because dEs are without bulges or disks, we will assume that the destruction of observable globular clusters due such shocks is minimal. However, if dEs possess central densities > 1 $M_\odot$ pc^{-3}, globular clusters passing through the central regions may experience some tidal stripping. Here we assume that dynamical friction is the dominant destruction mechanism.

The simplest hypothesis for the dE GCSs is that they started out with the same spatial and velocity distributions as the underlying stellar population. Durrell et al. (1996) summed the radial distributions for 11 dE GCS and found that dE GCS systems extended no more than 2.5 kpc from the galaxies' centers and followed the same distribution as the stellar light. However, an earlier study by Minniti et al. (1996) of the summed GCS of four Local Group dEs found evidence for more extended dE GCS. The GCS of giant galaxies are generally more spatially extended than the stars; no GCS has been found to be more centrally concentrated that the rest of the galaxy (Harris 1991). Because most GCSs are associated with a spatially extended component of galaxies, globular clusters could have formed before the bulk of the galaxy's star formation during a rapid monolithic collapse of proto-galactic halos. Another scenario predicting initially extended radial distributions suggests that globular clusters form from cool gas in the outer halo shocked by a starburst-driven galactic wind (Taniguichi, Trentham, & Ikeuchi 1999). However, the extended GCSs observed in giant ellipticals may result from the preferential destruction of globular clusters near the galaxy's center by bulge and disk shocking (Murali & Weinberg 1997; Vesperini 1997). Globular clusters may also form out of tidally shocked gas during galaxy mergers and strong interactions; observations of

forming star clusters in nearby mergers show that these clusters have the same radial distribution as the underlying stellar populations (Whitmore et al. 1993; Schweizer et al. 1996). For the purposes of this paper, we will assume that dE GCSs initially had the same spatial distribution as the host galaxy's stars.

Constraints on the structure of dE gravitational potential wells are particularly hard to come by, given the difficulty in observing such faint, generally low surface-brightness objects. Most studies have been limited to using the central stellar velocity dispersions (σ) of Local Group objects. Peterson & Caldwell (1993) find a tight correlation between the dE luminosity and σ, in agreement with supernovae-driven wind dE formation models (Dekel & Silk 1986). Bright dEs with $M_V \sim -17$ have $\sigma \sim 60$ km s^{-1} and faint dEs with $M_V \sim -12$ have $\sigma \sim 15$ km s^{-1}. Mass estimates from these velocity measurements assuming isotropic King profiles suggest that dEs are increasingly dominated by dark matter at fainter magnitudes (Aaronson 1983; Pryor & Kormendy 1990). However, the stellar velocity dispersion for some dEs are not isotropic - measurements of the anisotropy parameter $(v/\sigma)^*$ $(= \frac{v}{\sigma}/\sqrt{\epsilon/(1-\epsilon)}$, where v is the rotational velocity, σ is the mean velocity dispersion, and ϵ is the ellipticity at the radius where v is measured) yield values less than 0.4 (Bender & Nieto 1990). But the Bender & Nieto (1990) sample only contains two dEs and for simplicity we assume that dE dark matter halos are isotropic. Here we calculate the dynamical friction timescales for two isotropic potentials - the isothermal halo and the King model. We assume dEs to have circular velocities ($v_c = \sqrt{2}\sigma$ for the isothermal model, $v_c = \sqrt{3}\sigma$ for the King model) between 10-100 km s^{-1} for $M_V = -12$ to -17.

The time for the orbit of a globular cluster of mass M in an isothermal halo with a circular velocity v_c to decay from an initial radius r_i to the center is

$$t_{DF} = \frac{2.64 \times 10^2}{\ln\Lambda} \left(\frac{r_i}{2 \text{ kpc}}\right)^2 \left(\frac{v_c}{250 \text{ km s}^{-1}}\right) \left(\frac{10^6 \text{ M}_\odot}{\text{M}}\right) \text{Gyr} \quad (1)$$

(Binney & Tremaine 1987). If we assume that the globular cluster distribution generally follows the stellar light, the initial globular cluster radii should be comparable to dE half-light (effective) radii ($\sim$ 500 pc to 1.5 kpc, Peterson & Caldwell 1993).

The Coulomb logarithm $\ln\Lambda$ is given by

$$\ln\Lambda = \ln\left(\frac{\text{b}_{\max}\text{V}^2}{\text{G(M + m)}}\right), \quad (2)$$

where b_{max} is the maximum impact parameter between the cluster and interacting particle, V is the typical velocity of the system (for which we assume V $\sim v_c$) and m is the mass of the particle (star). The value of b_{max} for dE galaxies is unknown and may range between 0.5 to 3 kpc. However, this introduces only a 10-15 % uncertainty to the dynamical friction timescale. We assume $b_{max} =$ 1 kpc for all of our calculations.

Hernandez & Gilmore (1998) have recently re-addressed the dynamical friction timescales for dwarf galaxies, assuming dwarf dark matter halos are well represented by constant density core

region of a King distribution (King 1966). If the dark matter distribution has an approximately constant-density core with radius r_k, the dynamical friction timescale for clusters with $r_i = r_k$ becomes

$$t_{DF} = \frac{4}{3} v_c \left(\frac{r_k}{\mathrm{kpc}}\right)^2 \left(\frac{10^5\,\mathrm{M}_\odot}{\mathrm{M}}\right) \left(\frac{1}{\ln\Lambda}\right) \mathrm{Gyr}. \quad (3)$$

(Following Hernandez & Gilmore, here we have defined the "dynamical friction timescale" to be the time for the globular cluster orbit to decay to 1/16th of its initial radius.) The core radius of the King model is defined as $r_k = (9\sigma^2/4\pi G\rho)^{1/2}$. The light profiles of dEs are reasonably well fit by King models, although bright dEs tend to have central excesses (Binggeli & Cameron 1991). Typical stellar King core radii are on the order of 1 kpc. However, dEs are likely to be dark matter dominated and the extent of their dark matter halos is not well known. Pryor & Kormendy (1990) found the best dark matter models for the Draco and Ursa Minor dSphs were either isotropic with similar dark matter and stellar core radii or highly anisotropic with dark matter scale radii ≥ 10 stellar core radii. Dwarf spirals may also be fit with King profiles, but have larger dark matter core radii (2-8 kpc, Burkert 1995) .

In Figure 2, we plot the dynamical friction timescale as a function of circular velocity for dwarf-sized isothermal and King halos assuming different initial/ dark matter core radii and cluster masses. In the isothermal halo, clusters with masses $\geq 3 \times 10^5\ M_\odot$ and initial radii ≤ 1 kpc will spiral into the center in less than 10 Gyr. In the King halo, clusters with masses $\geq 2 \times 10^5\ M_\odot$ in a $r_k \leq 1$ kpc dark matter halo will spiral into the center in less than 10 Gyr. Thus, for simple yet reasonable assumptions, i.e. that dEs are adequately modeled by isotropic isothermal or King profiles, that the dark matter and initial globular cluster distributions follow the stellar profile, and that the clusters have ages similar to Galactic globular clusters (> 10 Gyr), the dE GCSs should be significantly affected by dynamical friction processes. The effects are stronger for fainter, lower mass dwarf galaxies.

4. Evolution of dE globular cluster radial distributions

As the orbits of globular clusters decay under dynamical friction, the massive clusters will sink into the center more quickly than the smaller clusters. We have run a simple Monte Carlo simulation to trace the evolution of the radial distribution of a typical dE globular cluster system. The simulation uses the analytic expression for radial decay due to dynamical friction in an isothermal sphere (Equation 1). Because dynamical friction decreases energy from a globular cluster at a rate proportional to dV^2 but decreases angular momentum at a rate proportional to dV, a globular cluster acting under dynamical friction will decay into orbits of maximum angular momentum (Hernandez & Gilmore 1998). Therefore we assume that the orbits of the globular clusters are circular. The clusters initially follow the exponential profile of the underlying stellar population and have the present day globular cluster mass function, independent of radius. The simulation

was run 100,000 times for three cases: $v_c = 50$ km s^{-1} and $r_0 = 2$ kpc; v_c =30 km s^{-1} and $r_0 = 1$ kpc; and v_c =15 km s^{-1} and $r_0 = 0.5$ kpc (Figure 3).

The simulated globular cluster radial profiles in Figure 3 demonstrate the increasing impact of dynamical friction on smaller, lower mass dwarfs. For the first two cases, dynamical friction has little effect on the summed profile of the entire GCS and only the massive clusters within the inner scalelengths fall into the galaxy's core within 10 Gyr. In the 50 km s^{-1} dE, all clusters with masses $> 5 \times 10^5\, M_\odot$ and radii < 1 kpc ($1/2\ r_0$) merge into the center within 10 Gyr. In the 30 km s^{-1} dE, all clusters with masses $> 5 \times 10^5\, M_\odot$ and initial radii < 2 kpc ($2\ r_0$) merge into the center within 10 Gyr. As the inner-most massive clusters are destroyed, some of the massive clusters originally found in the outer regions sink into the central few scalelengths. The remaining less massive and more extended clusters sink more slowly inwards and retain the exponential radial distribution in the outer regions of the dE. However, in the 15 km s^{-1}, 0.5 kpc simulation, after 10 Gyr $\sim 85\%$ of all clusters have merged into the center and 99.9% of $M_V < -8.0$ clusters have been destroyed. In the faintest and smallest dE, most of the globular clusters should merge to form a bright nucleus in less than a Hubble time.

We have examined the summed radial distribution of both the bright ($M_V < -8$), non-nucleus cluster candidates and the entire GCSs of our dE sample for evidence of these dynamical friction processes. Because our sample includes dEs with $-11.9 > M_B > -17.3$, we expect the impact of dynamical friction on our summed radial distribution will be most noticeable in the deficit of massive clusters in the inner regions of dE. For each dE, we typically detect only a few globular cluster candidates in excess of the background. Without radial velocities, it is impossible to determine if a given globular cluster candidate is associated with the dE or is a background galaxy or foreground star. Figure 4 shows the magnitude distribution of globular cluster candidates and background/foreground objects satisfying the same color and compactness criteria. Significant contamination by background objects affects the brightest bins; roughly 30% of the brightest cluster candidates which fall on chip 3 and have $M_V < -8$ are likely to be background objects. Assuming $M/L_V = 2$, a $M_V = -8$ cluster has a mass $\sim 2.5 \times 10^5\, M_\odot$. The dynamical friction timescale for a $2.5 \times 10^5\, M_\odot$ cluster with an initial radius of 1 kpc in an isothermal halo with $v_c \sim 40$ km s^{-1} is ~ 5 Gyr, thus the dynamical friction effects should be apparent for these bright clusters.

We have scaled the entire globular cluster system of each dE by the host galaxy's exponential scalelength r_0, subtracted out the background contamination, and summed the radial distributions of our 51 dEs to create a composite globular cluster radial distribution (top half of Figure 5). The nuclei are excluded from this radial distribution. The summed distribution was corrected for radial dependence on incompleteness, as determined in Figure 1b. This composite globular cluster radial profile is well fit by an exponential profile and follows the light profile of dEs:

$$\ln(\mathrm{N_{gc}/area}) = (-0.97 \pm 0.12) \times (\frac{r}{r_0}) + (4.76 \pm 0.45)\ (\mathrm{RMS} = 0.29). \qquad (4)$$

No deficit below the exponential profile for the entire summed globular cluster distribution is apparent; however, the effect of dynamical friction on the total distribution is likely to be undetectable

(Figure 3).

In the bottom of Figure 5, we have plotted the radial distribution of the bright ($M_V < -8.0$) non-nuclear cluster candidates, corrected for the 30% contamination, scaled by the exponential scalelength of the galaxy and summed over the entire dE sample. We have done no correction for incompleteness because the correction should be very small for clusters brighter than $M_V = -7.0$, even in the central regions of the dEs. The best linear fit to this profile is $\sim 4\sigma$ shallower than an exponential profile:

$$\ln(\mathrm{N_{gc}/area}) = (-0.68 \pm 0.07) \times (\frac{r}{r_0}) + (2.93 \pm 0.25) \ (\mathrm{RMS} = 0.21). \quad (5)$$

Thus, it appears that there is a significant deficit of bright, massive globular clusters in the inner regions of our sample dEs.

5. Formation of dE nuclei via dynamical friction

Our Monte Carlo simulation of the evolution of dE globular cluster systems' radial profiles shows that massive clusters quickly spiral into the centers of dE. The brightest globular cluster candidate in a dE is often the nucleus with $< M_V >= -10.3$ (M $\sim 3 \times 10^6$ $M_\odot$, assuming M/L_V =2). Most of the nuclei in our sample lie in a fairly small $(V - I)$ range between 0.85 and 1.10, consistent with a 12 Gyr stellar population and a metallicity range between 1/100 and 1/5 solar (Figure 6). The fainter nuclei are also found in fainter galaxies, which generally have fewer clusters overall (top of Figure 7). There is a slight color-magnitude relation where the fainter nuclei are bluer. One can imagine a scenario where fainter, less massive galaxies initially have fewer clusters and lower metallicities, and form fainter, bluer nuclei. The nuclei of FCC25 and FCC1714 lie outside of these trends. FCC 25 is ~ 0.4 magnitudes redder than the other nuclei and could be a background galaxy. FCC 1714 is ~ 0.3 magnitudes bluer and could also be a background/foreground object or a < 1 Gyr old cluster.

We ran another set of Monte Carlo simulations to predict the magnitude of each dE nucleus in our sample of dE,N based on each galaxy's intrinsic properties (Table 1). Again, the simulation randomly sampled the cluster mass function and an exponential radial distribution and allowed the clusters to orbitally decay for 5 Gyr. Any cluster with a final radius ≤ 0 was merged into the nucleus. The velocity dispersion σ was estimated using the σ - luminosity relation for dEs (Dekel & Silk 1987, Peterson & Caldwell 1993) and converted to circular velocity assuming $v_c = \sqrt{2}\sigma$. Each galaxy's exponential scalelength was measured from our HST WFPC2 I image (Table 1). The initial number of clusters was estimated by correcting the present day number of clusters by the dynamical friction destruction efficiency. The globular cluster destruction efficiency due to dynamical friction depends on the host galaxy's scalelength and circular velocity. dE,N with less than 2 detected clusters were excluded due to the uncertainty in calculating the globular cluster destruction efficiency. After 5 Gyr, $\sim 15\%$ of globular clusters will merge into a nucleus in a $v_c =$

50 km s^{-1}, $r_0 = 2$ kpc dE and $\sim 80\%$ of globular clusters will merge into a nucleus in a $v_c = 15$ km s^{-1}, $r_0 = 500$ pc dE. Note that, if dynamical friction is as efficient at destroying globular clusters as our simulations suggest, then the faintest dEs initially formed with up to ten times as many clusters as we observe today.

Assuming nuclei form via dynamical friction, we predict a much weaker trend of nuclear magnitude with galaxy magnitude than observed (bottom of Figure 7). While the fainter galaxies generally have fewer globular clusters from which to form nuclei, they should have shorter dynamical friction timescales and thus should be more efficient at destroying clusters and forming nuclei. However, our simulation over-predicts the mass of the nuclei in most of our sample. Figure 8 plots the predicted M_V magnitude of the nucleus vs. the observed M_V magnitude for each dE,N. Nuclei which fall on or below the solid line may have formed via dynamical friction processes within 5 Gyr. Thus, even the bright nucleus of VCC1254 ($M_V = -12.59 \pm 0.02$) may have been formed from the decayed remnants of massive globular clusters. However, many of the faint nuclei (found primarily in the $M_V > -14$ galaxies) are several magnitudes fainter than predicted.

Many of these faint galaxies have extremely high S_N (Tables 1 and 2) and possess extended GCS. Dynamical friction arguments would suggest that most of the clusters in these diffuse galaxies should have merged into a single bright nucleus and the globular cluster population we observe today is less than a third of the original population. Clearly, dynamical friction is not as effective at destroying globular clusters and forming nuclei in the faint dEs as our simple simulations predict. While the faint nuclei may have been formed via the orbital decay of massive globular clusters, some mechanism seems to have minimized the dynamical decay of the GCSs in these dEs.

6. Possible mechanisms working against dynamical friction

We have detected evidence for the action of dynamical friction in the radial distribution of the bright non-nuclear globular clusters in dE galaxies and found that the brightest nuclei are consistent with formation via the orbital decay of massive clusters in the center of the host dE. However, our Monte Carlo simulations of the formation of dE nuclei do not adequately reproduce the strong observed trend of decreasing nuclear luminosity with decreasing galaxy luminosity. In the faint dEs, some mechanism is working against dynamical friction to prevent the collapse of the entire globular cluster system. This result is reminiscent of the observations of the Fornax and Sagittarius dSph GCSs. Both of these $M_V > -14$ Local Group dSph possess high specific frequencies and extended GCSs, despite extremely short dynamical friction timescales. In this section we consider the mechanisms which may counteract or minimize the dynamical drag on the globular clusters in faint dE.

1) The globular clusters in the faintest dEs could be younger than their dynamical friction timescales (≤ 5 Gyr). Many Local Group dSph possess significant numbers of intermediate age stars (1-8 Gyr), and several "young" globular clusters (4-8 Gyr) are associated with the Sagittarius

and Fornax dSph (Grebel 1997, van den Bergh 2000). Combined with the existence of numerous faint blue galaxies in the field, this suggests that many dwarf galaxies experienced a secondary starburst between z $\sim$ 0.5 - 1.5. Although the dE globular clusters have colors and luminosities similar to the 12-14 Gyr globular clusters in our Galaxy, the age-metallicity degeneracy prevents us from constraining their ages to better than a few Gyr. However, for the Fornax dSph, where globular cluster ages can be constrained by color magnitude diagrams, the youngest globular cluster is still several Gyr older than its dynamical friction timescale (Oh, Lin, & Richer 2000).

2) dEs may have undergone significant mass loss due to supernovae-driven winds during the formation of their first stars. The fractional mass lost increases with decreasing mass, thus the smallest objects suffered the greatest mass loss (Dekel & Silk 1986). The galaxy's globular cluster system may have become more extended than the remaining stars as a result of the supernovae-driven wind, and take longer to spiral inward under the influence of dynamical friction. If they formed in the galaxy's halo before the onset of the wind (McLaughlin 1999) or as the wind shocked the galaxy's outer halo (Taniguichi et al. 1999), they would initially possess a radial profile more extended than the stellar light. The initial extent of this globular cluster halo may increase with increasing mass loss and decreasing initial mass. However, it is difficult to see how the GCSs could then evolve to match the exponential stellar profile at the present day.

3) The structure of the dark matter halos may be significantly different from the stellar halos. An increase in either the dark matter density or the dark matter core radius relative to the stellar density or core radius will increase the velocity dispersion of the dark matter and the dynamical friction timescale of the globular clusters (Hernandez & Gilmore 1998). The M/L estimates for dEs predict that most of the mass is in dark matter; thus the interaction with the dark matter rather than with the stars will dominate the drag on the globular clusters. The faintest dEs may have high dark matter densities (Dekel & Silk 1986; Peterson & Caldwell 1993) which would slow down the orbital decay of the clusters. The Local Group dSph show a trend towards increasing mass to light ratios with decreasing luminosity (Peterson & Caldwell 1993; Mateo 1998). Also, the distribution of dark matter in dEs is very poorly constrained. Dwarf spirals and other LSBs for which HI rotation curves may be measured show dark matter halos which extend several scalelengths beyond the stellar profiles. If dEs are gas-stripped dwarf irregulars and spirals, they too should have extended dark matter halos.

Expressing the dynamical friction time scale of Equation (3) in terms of the density (see also Carollo 1999 for a different derivation) yields for clusters starting with the core radius the relation

$$t_{DF} = \frac{1.26 \times 10^2}{\ln \Lambda} \left(\frac{r_k}{2 \text{ kpc}} \right)^3 \left(\frac{10^6 \mathrm{M}_\odot}{\mathrm{M}} \right) \left(\frac{\rho}{\mathrm{M}_\odot \mathrm{pc}^{-3}} \right)^{1/2} \text{Gyr}, \tag{6}$$

with the density given by $\rho_0 = 0.55 \ (\frac{V_0}{100 \text{ km s}^{-1}})^2 \ (\frac{1\text{kpc}}{r_k})^2 \ \mathrm{M}_\odot \ \mathrm{pc}^{-3}$. Our results would imply dE dark matter densities in excess of $\sim 1 \ \mathrm{M}_\odot \ \mathrm{pc}^{-3}$ or dE dark matter core radii > 2 kpc for the faintest dE.

Modified Newtonian Dynamics (MOND) offers a possible alternative to dark-matter dominated

dEs. MOND has been successful at explaining the velocity rotation curves of low surface brightness disk galaxies; dSph and dEs should also provide a strong test for MOND (McGaugh & de Blok 1998). However, a full derivation of dynamical friction taking into account the effects of MOND is needed to determine if MOND is consistent with our results and that is beyond the scope of this paper.

4) The clusters may be heated in such a way that counters their orbital decay via dynamical friction. Oh, Lin & Richer (2000) recently attempted to identify possible heating mechanisms for the Fornax dSph GCS. One possible mechanism for injecting kinetic energy into the GCS is by scattering of the globular clusters after close encounters with massive black holes ($M_{BH} \geq M_{GC}$). Such scattering may also occur once a massive nucleus has formed. However, repeated encounters are likely to destroy the clusters.

Oh et al. (2000) also examine the effects of the tidal disruption of the Fornax dSph by the Galaxy. While the tidal forces increase the globular cluster orbital eccentricities and velocity dispersions, the strong tidal forces can not increase the GCS kinetic energy enough to counter the dynamical friction drag. But, if Fornax has experienced significant mass loss (50-90 %) via tidal stripping over many internal dynamical timescales, the clusters will retain their energy in a shallower gravitational potential well and their orbital radii will increase, countering the drag of dynamical friction.

The dEs in our sample were selected to not be close companions of giant galaxies, for fear that the dE globular cluster candidates would be contaminated by those of the giant companion. However, the tidal field of the entire cluster of galaxies may play a role in heating their GCSs. Oh & Lin (2000) model the effects of the extra-galactic tidal field of the Virgo Cluster on dE GCSs. dEs within the inner regions of Virgo experience a relatively weak external tidal perturbation and therefore their GCSs are able to decay under dynamical friction and coalesce into nuclei. But in the outskirts of Virgo, dEs may be tidally disrupted and suffer significant mass loss as in the Fornax dSph simulation. Less massive galaxies are more likely to be disrupted and thus less likely to form nuclei.

7. Conclusions

We have examined high resolution HST WFPC2 V and I images of dE galaxies for evidence of dynamical friction in their globular cluster systems and nuclear properties. We find that, within the inner few scalelengths, our sample appears to be depleted of bright clusters, but there are no other observable effects on the summed profile. Monte Carlo simulations of the evolution of dE globular cluster systems show that the brighter nuclei may have formed via orbital decay into the galaxy's core. However, the observed trend of fainter nuclei in fainter galaxies is much stronger than expected if the nuclei form via simple dynamical friction processes. In these galaxies, some mechanism must be working against the orbital decay of the globular clusters. Mass loss via

supernova-driven winds, high dark matter densities and/or large dark matter cores, the formation of new star clusters, and tidal stripping may all conspire together to counteract the dynamical drag on the faintest dE GCSs and inhibit the formation of bright nuclei. We will obtain Cycle 9 HST WFPC2 observations of ~ 30 brighter dEs with larger GCS to improve our statistics.

We wish to thank Rosie Wyse and Brad Whitmore for useful discussions about dynamical friction and globular cluster detection. We also thank our referee, Tad Pryor, for his very constructive and helpful comments. Support for this work was provided by NASA through grants GO-06352.01-95A and GO-07377-01-96A from the Space Telescope Science Institute, which is operated by the Association of Universities for Research in Astronomy, Incorporated, under NASA contracted NAS5-26555.

REFERENCES

Aaronson, M. 1983, ApJ, 266, L11

Barnes, J. & Hernquist, L. 1992, Nature, 360, 715

Bender, R. & Nieto, J.L. 1990, A&A, 239, 97

Binggeli, B. & Cameron, L.M. 1991, A&A, 252, 27

Binggeli, B., Sandage, A., & Tammann, G.A. 1985, AJ, 90, 1681

Binney, J. & Tremaine, S. 1987, Galactic Dynamics, (Princeton: Princeton University Press)

Bothun, G. D. & Mould, J. R. 1988, ApJ, 324, 123

Buonanno, R., Corsi, C.E., Castellani, M., Marconi, G., Fusi Pecci, F., & Zinn, R. 1999, AJ, 118, 1671

Burkert, A. 1995, ApJ, 447, L25

Caldwell, N. & Bothun, G. D. 1987, AJ 94:1126.

Carollo, C. M. 1999, ApJ, 523, 566

Chandrasekhar, S. 1943, ApJ, 97, 255

Davies, J. I. & Phillips, S. 1988, MNRAS 233:553.

Dekel, A. & Silk, J. 1986, ApJ, 303, 39

Dominguez-Tenreiro, R. & Gomez-Flechoso, M.A. 1998, MNRAS, 294, 465

Durrell, P. R., Harris, W.E., Geisler, D., Pudritz, R.E. 1996, AJ, 112, 972

Fall, S.M. & Rees, M.J. 1977, MNRAS, 181, 37

Ferguson, H.C. & Sandage, A. 1988, AJ, 96, 1520

Ferguson, H.C., & Sandage, A. 1989, ApJ, 346, L53

Fusi Pecci, F., Bellazzini, M., Cacciari, C., & Ferraro, F.R. 1995, AJ, 110, 1664

Grebel, E. 1997, Rev. Mod. Astron., 10, 29

Harris, W. 1991, ARAA, 29, 543

Hernandez, X. & Gilmore, G., 1998, MNRAS, 297, 517

Hunsberger, S.D., Charlton, J. & Zaritsky, D. 1996, ApJ, 462, 50

James, P.A. 1994, MNRAS, 269, 176

King, I. 1966, AJ, 71, 64

Mateo, M. 1998 ARAA, 36, 435

McGaugh, S.S. , & de Blok, W.J.G. 1998, ApJ, 499, 66

McLaughlin, D. 1999, ApJ, 117, 2398

Miller, B.W., Lotz, J.M., Ferguson, H.C., Stiavelli, M., & Whitmore, B.C. 1998, ApJ, 508, L133

Miller, B.W., et al. 2001, in prep.

Minniti, D., Meylan, G., & Kissler-Patig, M. 1996, A&A, 312, 49

Mirabel, I.F., Dottori, H., & Lutz, D. 1992, A&A, 256L, 19

Montegriffo, P., Bellazzini, M., Ferraro, F.R., Martins, D., Sarajedini, A., & Fusi Pecci, F. 1998, MNRAS, 294, 315

Moore, B., Lake, G., & Katz, N. 1998, ApJ, 495, 139

Murali, C., & Weinberg, M. D. 1997, MNRAS, 288, 767

Oh, K.S., Lin, D.N.C., & Richer, H.B. 2000, ApJ, 531, 727

Oh, K.S., & Lin, D.N.C. 2000, ApJ, 543, 620.

Peterson, R.C., & Caldwell, N. 1993, AJ, 105, 1411

Pryor, C. & Kormendy, J. 1990, AJ, 100, 127

Sandage, A., Binggeli, B., & Tammann G.A. 1985, AJ, 90, 1759

Schweizer, F., Miller, B.W., Whitmore, B., Fall, S.M., 1996, AJ, 112, 1839

Taniguchi, Y., Trentham, N., & Ikeuchi, S. 1999, ApJ, 526, L13

Thuan, T.X. 1985, ApJ, 299 881

Tremaine, S.D., Ostriker, J.P., & Spitzer, L. 1975, ApJ, 196, 407

Tremaine, S. & Weinberg, M. 1984, MNRAS, 209, 729

van den Bergh, S. 1995, AJ, 110, 2700

van den Bergh, S. 2000, ApJ, 530, 777

Vesperini, E. 1998, MNRAS, 287, 917

Whitmore, B.C. & Schweizer, F. 1995, AJ, 109, 960

Whitmore, B.C., Schweizer, F., Leitherer, C., Borne, K., & Robert, C. 1993, AJ, 106, 1354

This preprint was prepared with the AAS LaTeX macros v5.0.

Table 1. Nucleated Dwarf Elliptical Galaxies [1]

Galaxy	Type	M_B [2]	M_V	Cycle	M_{Vnuc}	V-I_{nuc}	$r_0(''$)	r_0(kpc)	N_{gc}	S_N [3]
VCC1073	dE3,N	-17.0	-17.4	6	-11.62 ± 0.03	1.08 ± 0.04	8.6 ± 0.5	0.71 ± 0.04	18.8 ± 6.2	2.1 ± 0.7
FCC136	dE2,N	-16.6	-17.2	6	-11.50 ± 0.03	1.07 ± 0.04	8.4 ± 1.3	0.77 ± 0.12	20.1 ± 5.6	2.7 ± 0.8
VCC1876	dE5,N	-16.3	-16.6	6	-10.74 ± 0.03	1.00 ± 0.04	10.5 ± 0.3	0.86 ± 0.03	24.7 ± 6.8	5.5 ± 1.6
VCC1254	dE0,N	-16.2	-16.5	6	-12.59 ± 0.02	1.04 ± 0.04	7.7 ± 0.2	0.63 ± 0.02	24.6 ± 8.2	6.2 ± 2.2
FCC324	dS01(8)	-16.1	-16.4	6	-8.95 ± 0.04	0.91 ± 0.06	13.9 ± 0.3	1.30 ± 0.04	12.0 ± 4.8	3.3 ± 1.4
FCC150	dE4,N	-15.7	-16.2	6	-11.11 ± 0.03	1.05 ± 0.04	5.5 ± 0.3	0.51 ± 0.03	7.4 ± 4.2	2.4 ± 1.4
VCC452	dE4,N	-15.4	-15.8	6	-8.85 ± 0.04	0.94 ± 0.06	7.8 ± 0.4	0.64 ± 0.04	11.4 ± 5.8	5.3 ± 2.7
FCC316	dE3,N	-15.1	-15.2	6	-9.62 ± 0.03	1.08 ± 0.05	8.2 ± 0.3	0.75 ± 0.03	17.8 ± 5.7	14.6 ± 4.9
FCC174	dE1,N	-14.7	-15.3	6	-9.90 ± 0.03	0.93 ± 0.05	4.9 ± 0.5	0.45 ± 0.05	9.8 ± 3.8	7.2 ± 2.9
VCC503	dE3,N	-14.4	-14.5	6	-9.43 ± 0.03	0.89 ± 0.05	6.3 ± 0.4	0.52 ± 0.03	1.7 ± 3.6	2.8 ± 6.0
FCC254	dE0,N	-13.8	-14.7	6	-10.70 ± 0.03	0.92 ± 0.04	10.5 ± 0.5	0.97 ± 0.05	5.7 ± 4.1	7.7 ± 5.7
FCC25	dE0,N	-13.7	···	7	-9.80 ± 0.03	1.37 ± 0.04	6.1 ± 0.3	0.57 ± 0.03	5.2 ± 3.7	8.2 ± 5.8
VCC896	dE3,N	-13.4	···	7	-8.60 ± 0.04	1.01 ± 0.09	8.8 ± 0.6	0.75 ± 0.05	5.8 ± 3.9	12.0 ± 8.1
LGC50	dE,N	-13.3	-14.0	6	-8.90 ± 0.03	0.82 ± 0.05	10.2 ± 0.4	0.54 ± 0.02	5.5 ± 3.1	13.9 ± 9.2
VCC240	dE2,N	-13.0	-13.9	6	-9.89 ± 0.03	0.91 ± 0.04	9.5 ± 1.0	0.78 ± 0.08	8.6 ± 4.1	23.6 ± 14.
VCC529	dE4,N	-13.0	···	7	-9.85 ± 0.03	0.92 ± 0.04	6.6 ± 0.5	0.56 ± 0.05	3.5 ± 3.6	10.4 ± 10.9
VCC1530	dE2,N	-12.9	···	7	-9.90 ± 0.03	0.88 ± 0.04	5.9 ± 0.3	0.50 ± 0.03	7.5 ± 4.2	28.6 ± 13.5
VCC1783	dE5,N	-12.8	···	7	-9.15 ± 0.03	0.95 ± 0.05	11.6 ± 0.4	0.95 ± 0.03	0 ± 3.5	0 ± 13.9
VCC1714	dE4,N	-12.7	···	7	-12.03 ± 0.02	0.58 ± 0.03	12.0 ± 0.8	1.02 ± 0.07	0.6 ± 3.4	2.3 ± 13.5
VCC1272	dE1,N	-12.7	···	7	-7.84 ± 0.06	0.87 ± 0.09	4.2 ± 0.4	0.35 ± 0.04	1.7 ± 3.5	6.9 ± 14.1
FCC238	dE5,N	-12.7	···	7	-9.27 ± 0.05	0.91 ± 0.04	7.0 ± 0.7	0.65 ± 0.07	2.3 ± 2.0	9.2 ± 8.0
FCC189	dE4,N	-12.6	···	7	-9.12 ± 0.03	0.83 ± 0.05	2.4 ± 0.3	0.22 ± 0.03	1.2 ± 3.3	5.5 ± 15.9
VCC1252	dE0,N	-12.4	···	7	-9.21 ± 0.03	0.90 ± 0.05	4.7 ± 0.5	0.39 ± 0.04	6.3 ± 3.8	33.2 ± 20.0
VCC1363	dE3,N	-12.2	···	7	-8.98 ± 0.03	0.93 ± 0.05	3.7 ± 0.2	0.30 ± 0.02	0 ± 2.2	0 ± 15.2
VCC1077	dE0,N	-12.0	···	7	-8.69 ± 0.04	0.94 ± 0.06	3.3 ± 0.3	0.28 ± 0.03	1.2 ± 3.9	8.7 ± 29.4
FCC59	dE0,N	-12.0	···	7	-8.69 ± 0.04	0.85 ± 0.06	11.0 ± 2.2	1.02 ± 0.20	0 ± 3.1	0 ± 25.8
FCC146	dE4,N	-11.9	···	7	-8.06 ± 0.05	1.04 ± 0.08	3.3 ± 0.4	0.31 ± 0.04	1.7 ± 2.9	15.7 ± 26.6

[1] Cycle 6 data also presented in Miller et al. 1998.

[2] from Ferguson & Sandage 1990

[3] $S_N = N_{gc} \times 10^{0.4(M_V+15.0)}$, M_V assumed to be $M_B - 0.8$ where M_V not measured.

Table 2. Non-nucleated Dwarf Elliptical Galaxies [1]

Galaxy	Type	M_B [2]	M_V	Cycle	$r_0('')$	r_0(kpc)	N_{gc}	S_N [3]
VCC9	dE1,N?	-17.3	-17.5	6	18.3 ± 0.6	1.54 ± 0.05	22.9 ± 6.3	2.3 ± 0.7
VCC917	dE6	-16.3	-16.3	6	6.0 ± 0.2	0.50 ± 0.01	6.8 ± 5.3	2.1 ± 1.6
VCC118	dE3	-15.6	-15.3	6	8.0 ± 0.6	0.67 ± 0.05	3.4 ± 3.7	2.5 ± 2.7
VCC1577	dE4	-15.4	-15.8	6	7.1 ± 0.4	0.59 ± 0.03	14.9 ± 5.5	7.3 ± 2.8
LGC47	dE	-15.1	-15.5	6	12.9 ± 0.6	0.68 ± 0.03	3.5 ± 3.9	2.2 ± 2.4
VCC1762	dE6	-15.0	-15.2	6	6.9 ± 0.2	0.58 ± 0.02	4.0 ± 3.7	3.4 ± 3.1
FCC110	dE4	-14.6	-14.9	6	10.8 ± 0.4	0.99 ± 0.03	0 ± 3.8	0 ± 4.2
FCC48	dE3	-14.3	-14.8	6	6.9 ± 0.4	0.63 ± 0.04	5.1 ± 4.4	6.1 ± 5.3
VCC1651	dE5	-14.2	-14.6	6	19.2 ± 1.1	1.61 ± 0.09	1.1 ± 3.9	1.6 ± 5.7
FCC64	dE5	-13.9	-14.2	6	8.3 ± 0.7	0.77 ± 0.06	0 ± 2.6	0 ± 5.4
FCC212	dE1?	-13.8	···	7	15.1 ± 0.8	1.39 ± 0.07	6.9 ± 4.2	10.0 ± 6.1
FCC242	dE5	-13.6	···	7	9.3 ± 0.6	0.85 ± 0.05	0 ± 2.2	0 ± 4.2
VCC1729	dE5?	-13.4	···	7	6.3 ± 0.4	0.53 ± 0.03	1.2 ± 3.0	2.4 ± 6.3
VCC2029	dE3	-13.0	-13.9	6	5.0 ± 0.3	0.42 ± 0.02	1.1 ± 3.6	3.1 ±10.4
FCC218	dE4	-12.9	···	7	5.6 ± 0.5	0.51 ± 0.05	0 ± 2.6	0 ± 9.4
VCC996	dE5	-12.8	···	7	7.0 ± 0.4	0.59 ± 0.03	1.7 ± 3.2	6.2 ±11.8
VCC1877	dE2	-12.6	···	7	7.4 ± 0.2	0.62 ± 0.02	4.0 ± 3.2	17.6 ±14.1
FCC304	dE1	-12.6	···	7	7.2 ± 0.9	0.66 ± 0.09	0 ± 2.8	0 ± 13.4
VCC1781	dE4	-12.5	···	7	5.6 ± 0.4	0.47 ± 0.04	4.0 ± 3.2	19.3 ±15.5
VCC646	dE3	-12.4	···	7	5.6 ± 0.2	0.47 ± 0.02	6.3 ± 3.8	33.1 ± 20.
FCC246	dE2	-12.3	···	7	6.6 ± 0.7	0.61 ± 0.07	0 ± 2.6	0 ± 13.4
FCC144	dE0	-12.2	···	7	3.7 ± 0.4	0.34 ± 0.04	0.6 ± 3.4	3.6 ± 21.4
FCC27	dE2	-12.1	···	7	3.6 ± 0.5	0.33 ± 0.04	0 ± 2.8	0 ± 21.2
VCC607	dE7	-12.0	···	7	7.2 ± 0.7	0.60 ± 0.06	0 ± 2.7	0 ± 22.5

[1] Cycle 6 data also presented in Miller et al. 1998.

[2] from Ferguson & Sandage 1990

[3] $S_N = N_{gc} \times 10^{0.4(M_V+15.0)}$, M_V assumed to be $M_B - 0.8$ where M_V not measured.

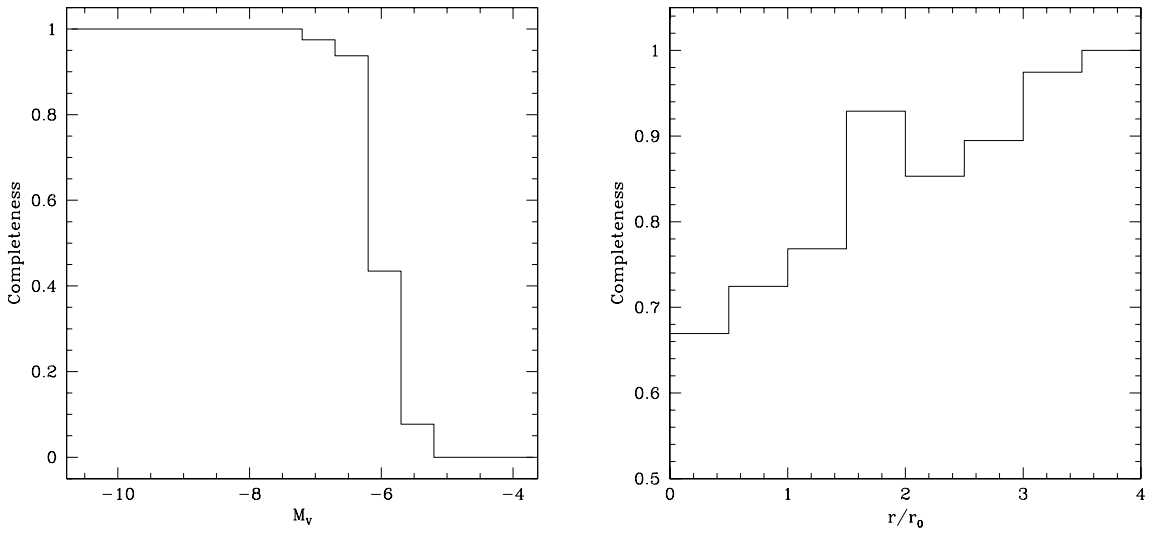

Fig. 1.— Completeness of the globular cluster detection as a function of globular cluster luminosity and distance from host galaxy center for a $V = 15.2$, $r_0 = 15\ ''$ dE (M_V = -16.0 at the distance of Virgo).

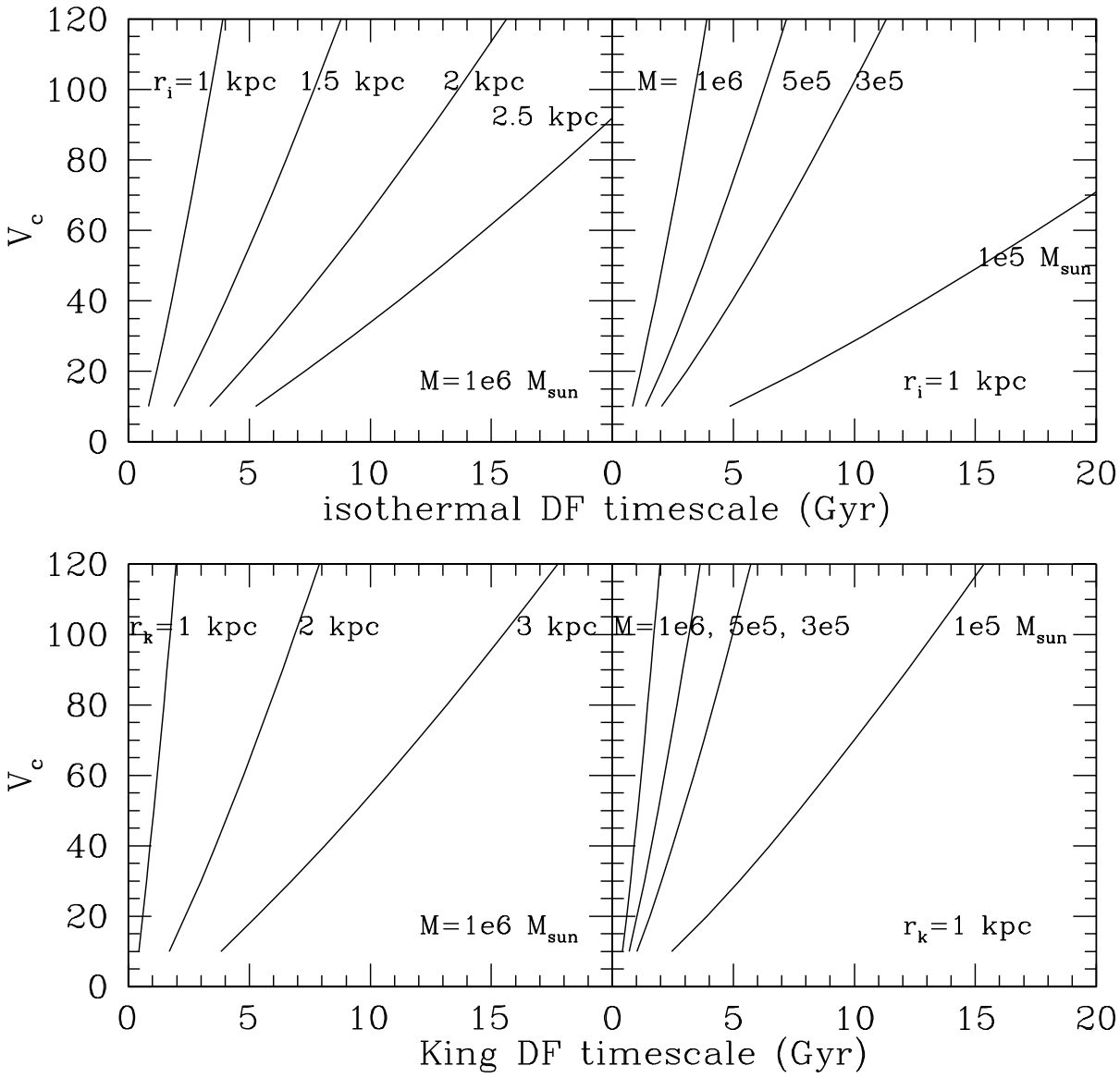

Fig. 2.— The dynamical friction timescale for dwarf-sized isothermal and King halos as a function of circular velocity.

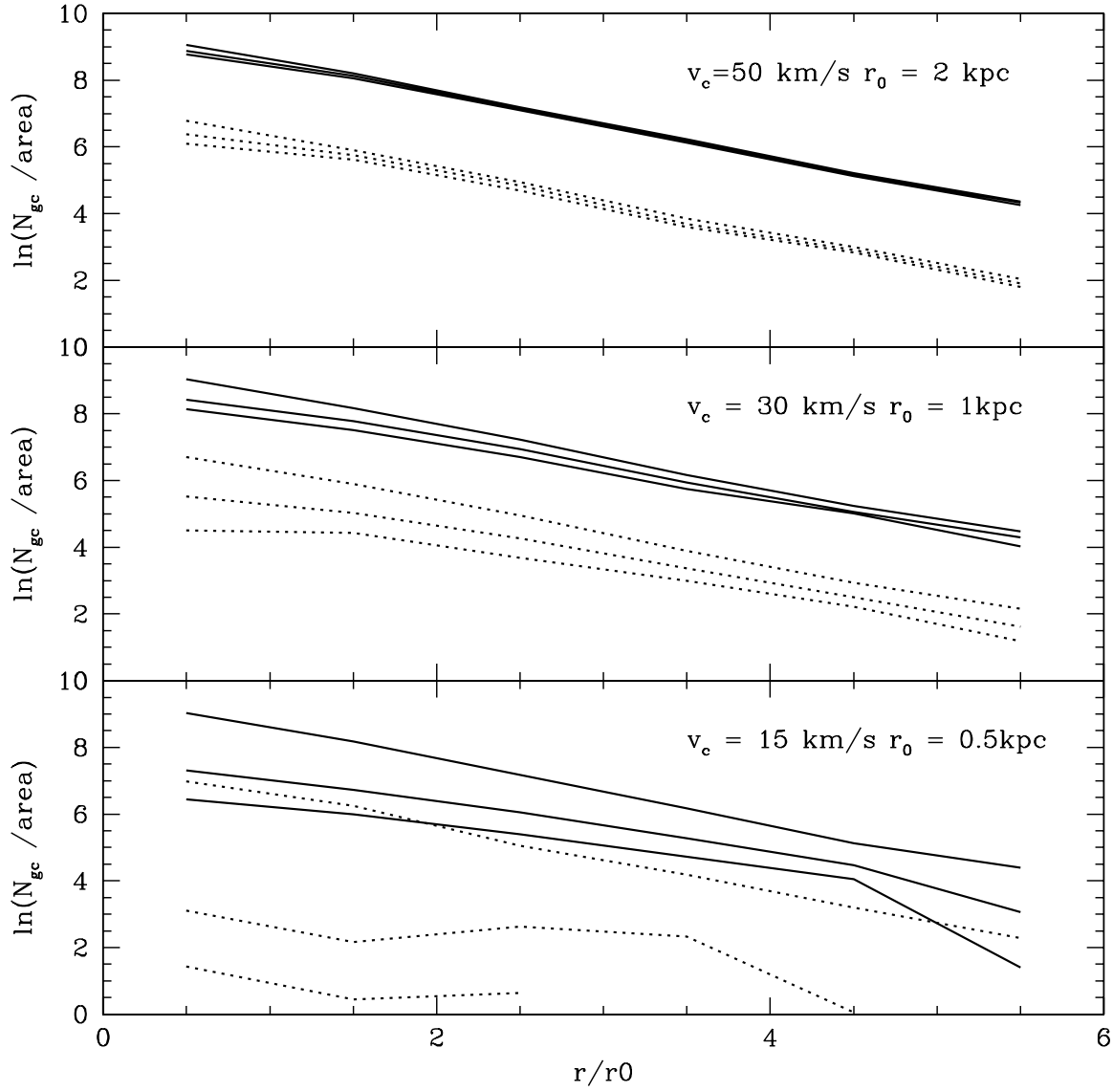

Fig. 3.— The evolution of the entire (solid lines) and bright ($M_V < -8$) (dashed lines) globular cluster radial profiles under the influence of dynamical friction in an isothermal halo after 0 (top line), 5 (middle), and 10 (bottom) Gyr.

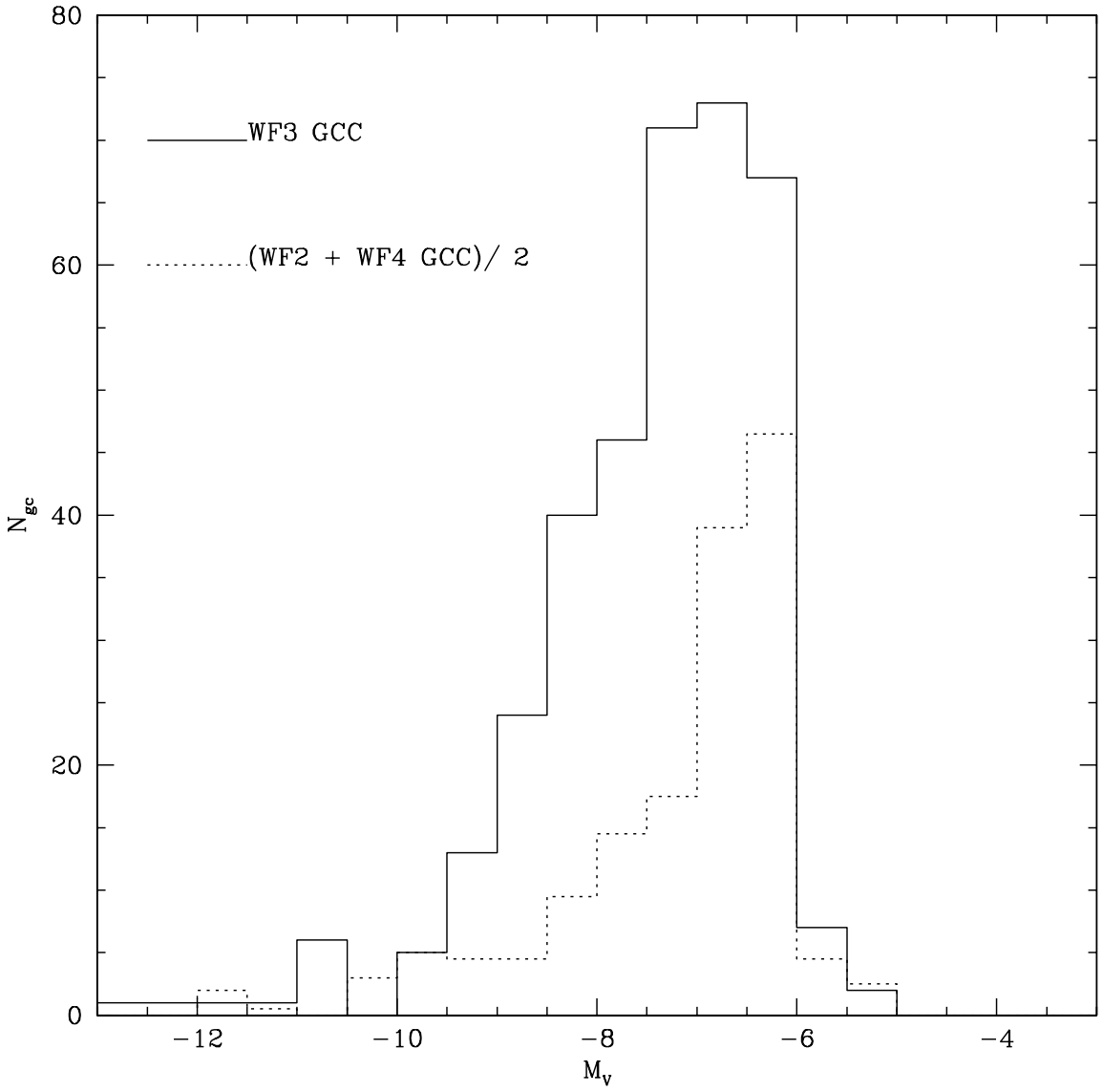

Fig. 4.— The luminosity distribution of Fornax and Virgo dE globular cluster candidates (solid line) and background objects (dashed line) for which $0.5 < (V-I) < 1.5$ and $FWHM < 2.5$ pixels.

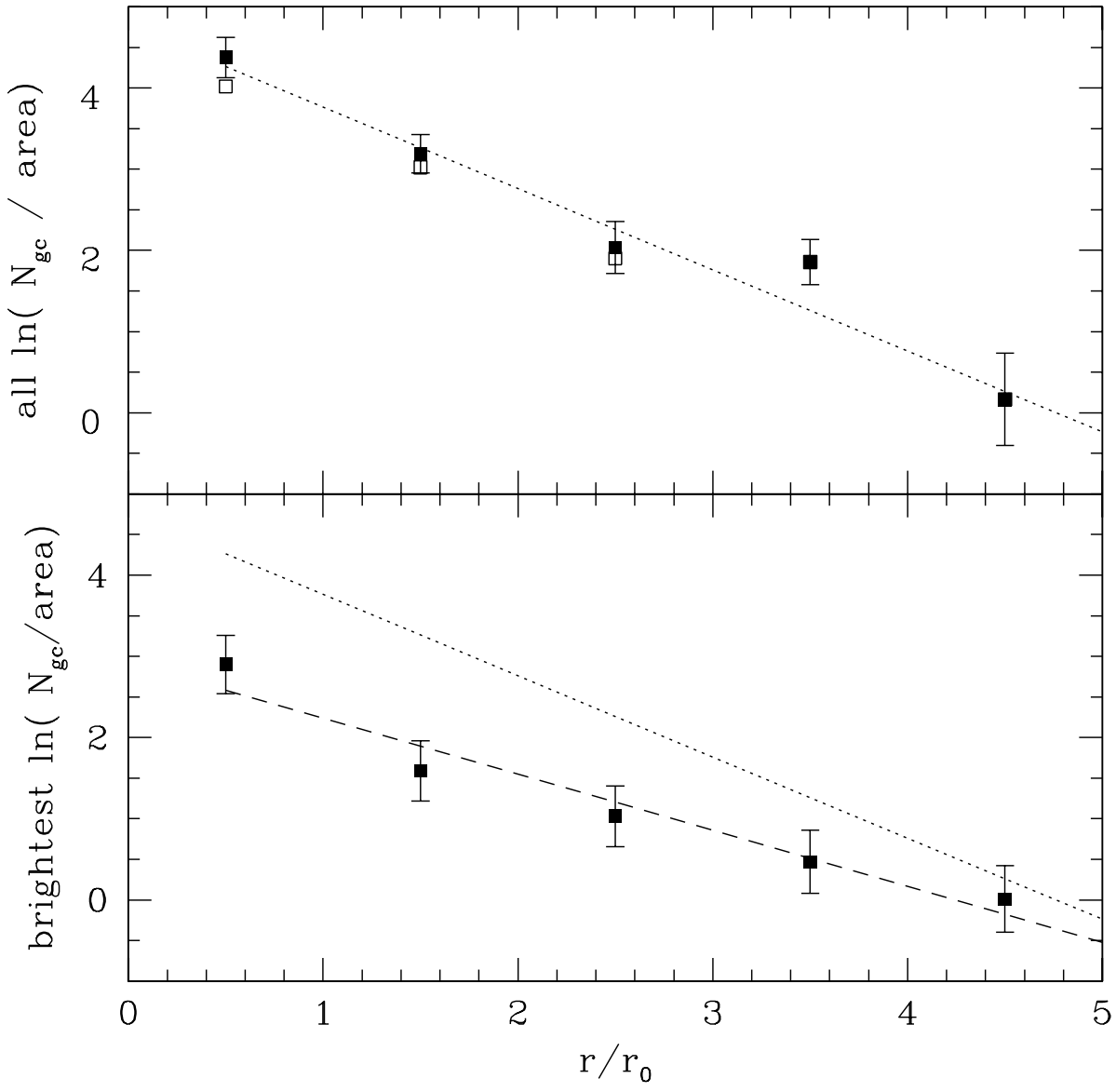

Fig. 5.— The summed radial distribution of the globular cluster candidates, corrected for background contamination, scaled by scalelength of galaxy, and excluding possible nuclei. The total globular cluster surface density (upper panel) follows the exponential light profile of the dEs (dotted line), but the bright clusters ($M_V < -8.0$, lower panel) appear to be depleted and have a shallower profile (dashed line). The open boxes in the top panel show the summed profile prior to correction for incompleteness effects in the inner regions. The error bars are $\sqrt{(N_{gc})^2 + (N_{background})^2}/area$.

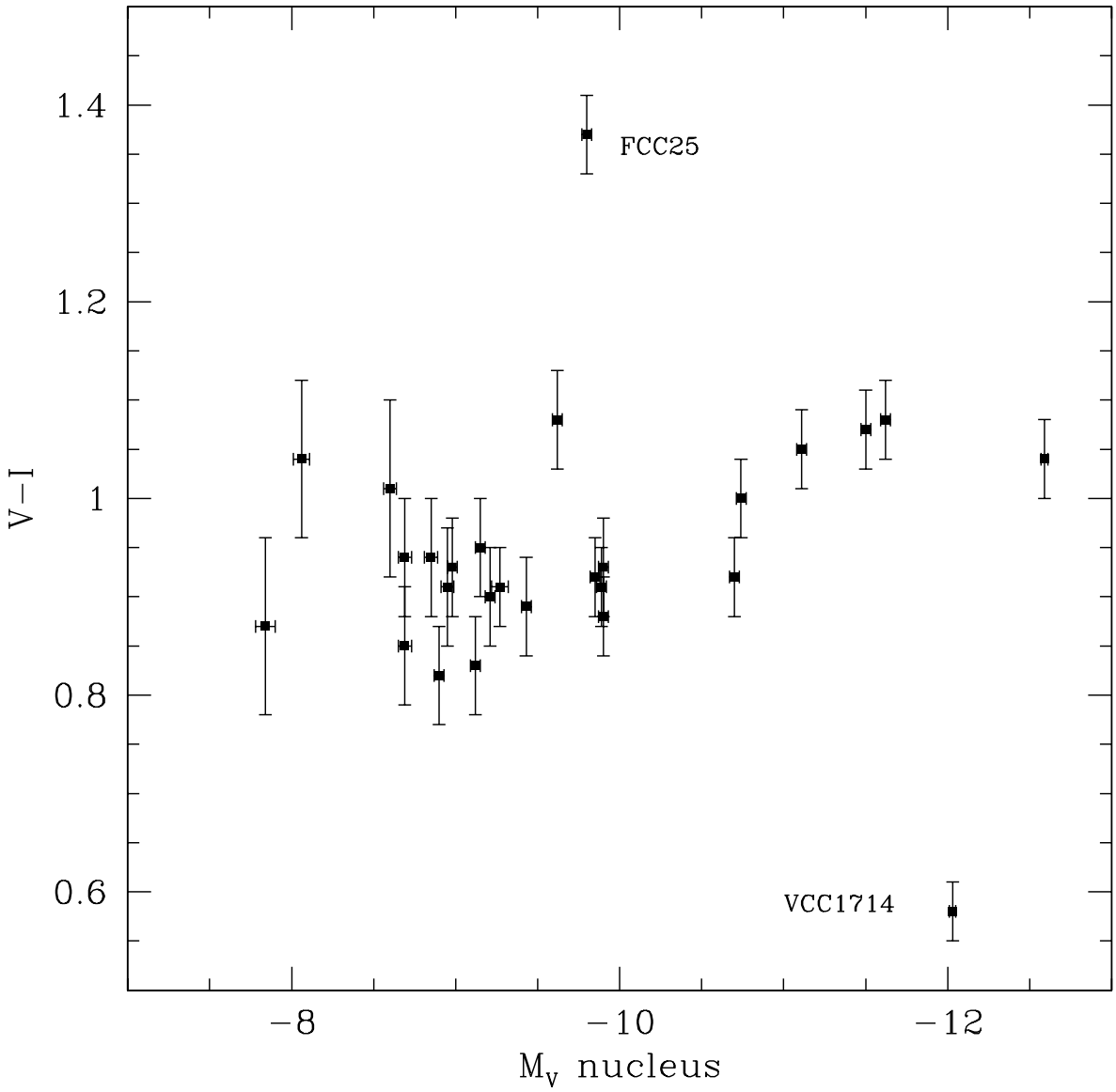

Fig. 6.— M_V vs. $V - I$ for the dE nuclei. Most nuclei have colors similar to old metal-poor Galactic globular clusters and have a slight trend towards redder colors with increasing luminosity. The nucleus of FCC25 is ~ 0.4 magnitude redder than the rest of the nuclei and could be a background galaxy. The nucleus of VCC1714 is ~ 0.3 magnitudes bluer than the rest of the nuclei and is consistent with an age < 1 Gyr.

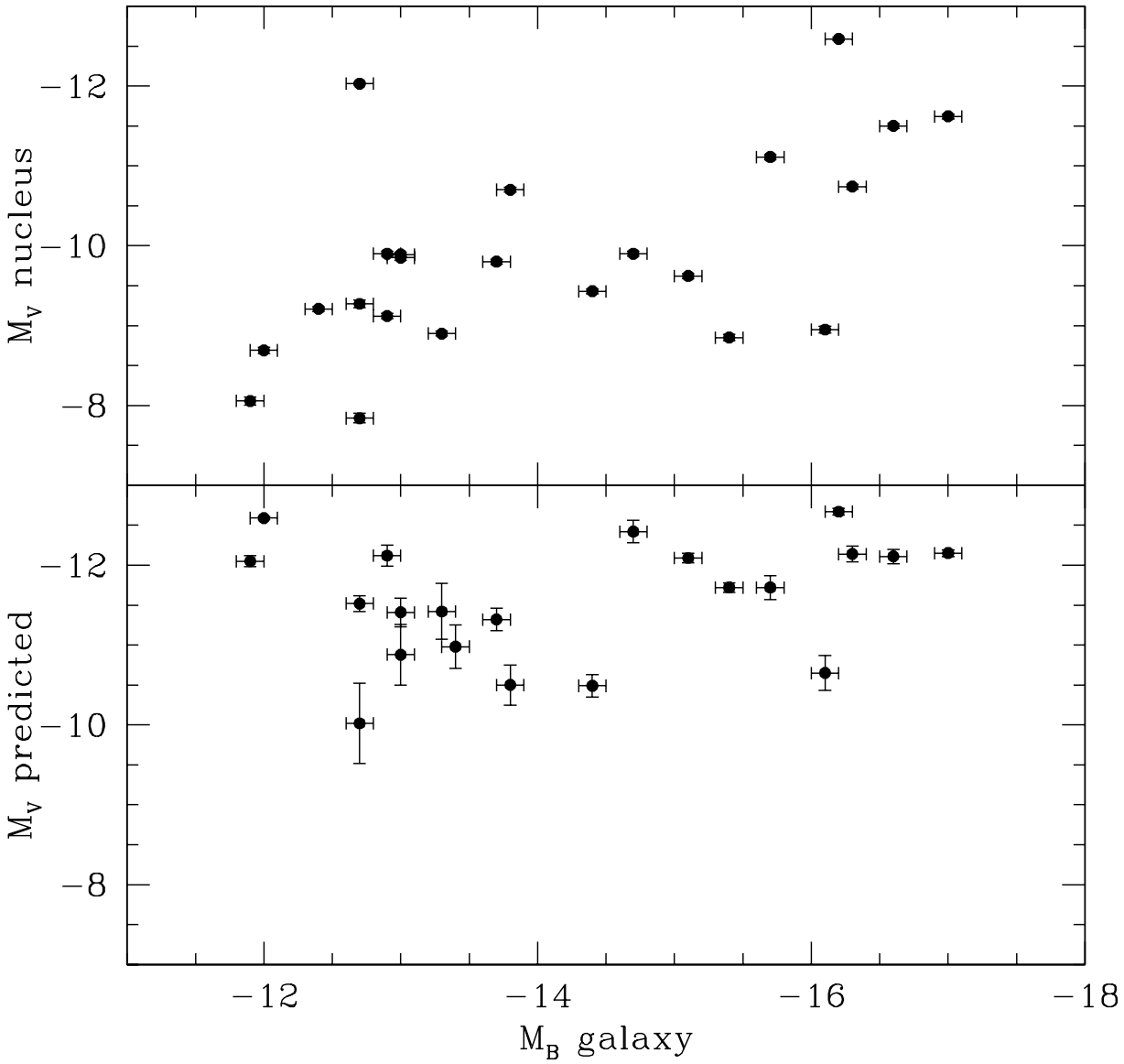

Fig. 7.— M_V of dE nuclei vs. M_B of host galaxy. Fainter galaxies tend to have fainter nuclei (top). Our simulation of dE nucleus formation (bottom) predicts a much weaker trend of nuclear luminosity with host galaxy luminosity.

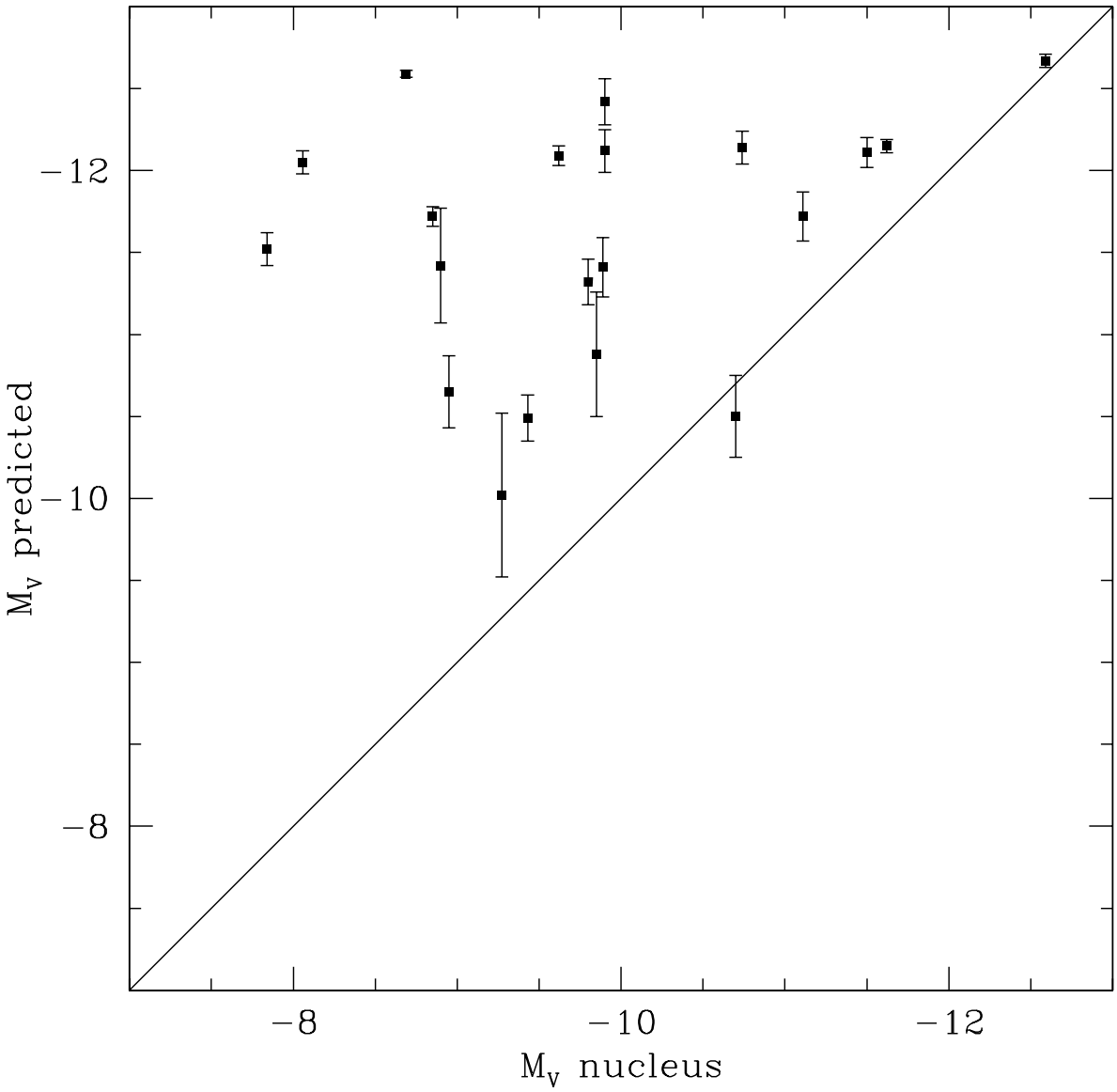

Fig. 8.— The predicted nuclear M_V from our Monte Carlo dynamical friction simulation vs. the observed nuclear M_V for each dE,N in our sample. We overestimate the nuclear M_V for dE with $M_B > -14$ by several magnitudes. The error bars are the standard deviation of the predicted magnitude for 100,000 trials. The standard deviation increases for galaxies with smaller globular cluster systems because of the random sampling of the globular cluster mass function.